

## Nonlinear mechanosensation in fiber networks

Estelle Berthier<sup>1</sup>, Haiqian Yang<sup>2</sup>, Ming Guo<sup>2</sup>, Pierre Ronceray<sup>3,\*</sup>, and Chase P. Broedersz<sup>1,4,†</sup><sup>1</sup>Arnold-Sommerfeld-Center for Theoretical Physics and Center for NanoScience,  
Ludwig-Maximilians-Universität München, D-80333 München, Germany<sup>2</sup>Department of Mechanical Engineering, Massachusetts Institute of Technology, Cambridge, Massachusetts, USA<sup>3</sup>Aix Marseille Univ, CNRS, CINAM, Turing Center for Living Systems, Marseille, France<sup>4</sup>Vrije Universiteit Amsterdam, Department of Physics and Astronomy, 1081 HV Amsterdam, Netherlands

(Received 31 March 2023; accepted 20 December 2023; published 26 March 2024)

In the extracellular matrix, eukaryotic cells exert forces that deform their surroundings. By doing so, they can perform mechanosensation: Cells measure the mechanics of their environment, and adapt their behavior accordingly. Extracellular matrices are, however, disordered nonlinear media: How can a mechanosensor at the cellular scale reliably measure the surroundings mechanics through local probing? Here, we develop a model for nonlinear mechanosensation in disordered fiber networks. At low forces, the linear response of the matrix combined with its extreme mechanical heterogeneity precludes reliable mechanosensation. In contrast, we find that this heterogeneity is strongly suppressed in the physiologically relevant nonlinear mechanical regime where fibers buckle. Conceptually, nonlinearity increases the range of mechanosensation, thereby enhancing disorder averaging and providing more accurate nonlinear mechanical measurements. We support our model using microrheology experiments and show theoretically that this nonlinear mechanosensation is generic to all fiber networks. This contrasts with the collagen-specific observation that nonlinear macroscopic elastic moduli are independent of network density, which we show to originate from the fiber's constitutive nonlinearity. Together, our theoretical study disentangles the micro- and macrorheological nonlinearities of fiber networks, and shows how mechanosensors such as cells can take advantage of these nonlinearities to robustly measure their mechanical environment despite heterogeneities.

DOI: [10.1103/PhysRevResearch.6.013327](https://doi.org/10.1103/PhysRevResearch.6.013327)

Cell behavior is steered by various cues from their extracellular environment. Such cues include chemical, electrical, and topographic signals that regulate key cell functions such as migration [1] and thereby impact processes ranging from embryonic development [2–4] and tissue maintenance to disease progression [5,6]. In particular, there is growing evidence for mechanosensation: Cells sense and respond to the mechanical properties of their environment [5,7–10]. The stiffness of the cell's substrate can guide developmental processes *in vivo*, such as axonal growth [11]. *In vitro* model systems further revealed that cells mechanically probe their substrate and subsequently modify behaviors such as differentiation [12], gene expression [13], and motility [14–16]. It remains unclear, however, what mechanical information cells can perceive inside the complex environments they encounter naturally [17,18].

*In vivo*, many cell types mechanically interact with the extracellular matrix (ECM) by adhering to network fibers and

exerting local forces. The polymerization and gelation processes through which these collagenous matrices form result in an inherently disordered fiber network with large structural variations at the cellular scale [19,20]. Consequently, the mechanical properties a cell-scale mechanosensor can locally measure depend strongly on network location [21–26]. This implies that cells face a highly heterogeneous mechanical environment [27,28] in which the cell-scale linear stiffness, measured at different locations in a single network, exhibits relative variations as large as between the macroscopic stiffness of tissues as distinct as brain (1 kPa) and bone (100 kPa) [22]. Thus, even if cells had ideal mechanosensors that could perfectly measure the local linear mechanical response, their ability to perform mechanosensation would remain limited by matrix disorder. Importantly, however, cells can exert forces of up to few nanonewtons [29–32] to probe their environment, easily exceeding the linear response regime of the ECM [33–35]. Indeed, collagen networks exhibit a pronounced nonlinear response at relatively small stresses or deformations. Understanding how such nonlinearities impact mechanosensation at the scale of a cell inside the disordered ECM is the primary goal of this article.

The macroscopic nonlinear behavior of disordered fiber networks is well characterized both theoretically [36–43] and experimentally [44–50]. Nonlinearities arise through a range of effects, including constituent nonlinearities such as fiber buckling [51] and entropic stiffening [39,47,52], or

\*pierre.ronceray@univ-amu.fr

†c.p.broedersz@vu.nl

network nonlinearities arising from their low connectivity [53–55]. By contrast, the nonlinear mechanics of the network in response to local probes at scales relevant to how a cell mechanically interacts with the ECM remains poorly understood [21,23,43,56–58]. As the force is increased, fiber buckling occurs and marks the transition from a bending- to a stretching-dominated response [59]. A nonlinear region thus emerges in the vicinity of a local probing force [33,52], where fiber buckling and associated fiber alignment, facilitated by the removal of orthoradial constraints, result in a stress decay that is slower than in linear elasticity, consistent with cell-generated displacement fields [35]. Recent discrete and continuous theoretical approaches established the role of buckling in the formation of this region [60–63], determined its spatial range [62–64], and its impact on stress transmission [62,65]. To investigate the ability of a cell-scale mechanosensor to infer matrix mechanics using local force probes, we thus need to understand the interplay between these nonlinearities and the structural disorder of the network.

Here, we theoretically investigate the relation between bulk and local nonlinear elasticity to elucidate the ability of an ideal mechanosensor at the cellular scale to measure the nonlinear mechanical properties inside a disordered fiber network. First, we derive a simple relation describing how the fiber constituent stiffening and density control the macroscopic nonlinear mechanics, which explains the unique density independence of the nonlinear stiffness of collagen networks [44]. Surprisingly, however, we find that these macroscopic nonlinear properties do not control the local nonlinear mechanical properties. The local mechanical response measurable by an ideal mechanosensor is strongly modulated by variations in fiber density, although the relative variations in the mechanics decrease with force as the response becomes nonlinear. Using both theory and experiments, we discover a generic power-law decay of the relative variability of local mechanical measurements with force. This power law controls how the local nonlinear mechanical response becomes increasingly insensitive to network disorder for a range of fiber constitutive nonlinearities. To provide insights, we develop a simple model for this concept that we term nonlinear mechanosensation. Our model shows how large probing forces applied by a local mechanosensor induce fiber buckling over an extended range, thereby effectively enhancing the length-scale over which a mechanical measurement is averaged in a disordered network. Thus, we here find that elastic nonlinearities can be exploited by mechanosensors, such as cells, to overcome the inherent disorder of their environment and making it possible to use local measurements to infer the macroscopic mechanical properties of the ECM.

## I. MODEL FOR DISORDERED NONLINEAR FIBER NETWORKS

To investigate the consequences of structural heterogeneity in fiber networks on the local mechanical environment an ideal mechanosensor can measure, we build on a broadly used minimal model for a disordered fibrous matrix [38,66]. In this model (see Materials and Methods), we introduce structural disorder by randomly depleting bonds on a regular lattice. The lattice fibers are represented by these bonds that are present

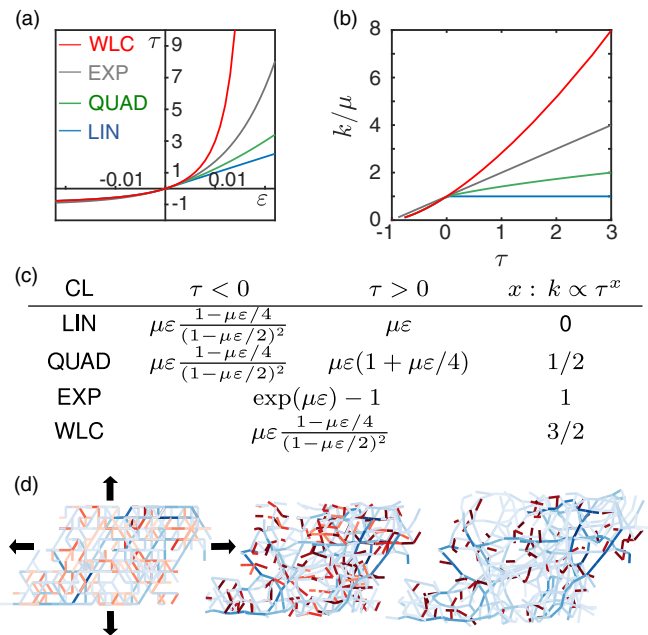


FIG. 1. Nonlinear fiber network model. Constitutive law (CL) of the fibers, (a) bond tension ( $\tau$ ) vs deformation ( $\epsilon$ ), (b) corresponding bond differential stiffness ( $k$ ), normalized by the linear modulus ( $\mu$ ) as a function of its tension, (c) mathematical expression of CLs. (d) Macroscopic loading of a 3D EXP-fiber network with  $p = 0.35$  at three dilatation strains  $\gamma = 10^{-5}$ ,  $8 \times 10^{-2}$  and  $2 \times 10^{-1}$ . Color code: low to high tensile forces (resp. compressive forces) from light to dark blue (resp. red).

with a probability  $p$ , setting the fiber density. Fiber bonds resist both bending and longitudinal deformations. Here, we describe the longitudinal fiber response with a nonlinear force-extension constitutive law (CL)  $\tau = f(\epsilon)$ , with  $\epsilon$  the fiber's relative longitudinal deformation and  $\tau$  its tension. This CL is chosen to be asymmetric in compression and tension. Indeed, fibers buckle and soften under compression ( $\epsilon < 0$ ) and can stiffen beyond a characteristic tension, with a power law increase  $k \propto \tau^x$  of their differential stiffness  $k = d\tau/d\epsilon$ , where the exponent  $x$  characterizes the stiffening mechanism.

The exponent  $x$  is varied to assess the effects of the nonlinear fiber micromechanics on mechanosensing. The values are selected to capture the mechanical behavior of various biopolymers employed in experiments, in particular collagen, the main ECM constituent [20]. Indeed, the case  $x = 1$ , corresponds to an exponential CL [EXP, Figs. 1(a)–1(c)], reflecting the empirically established stress-strain relationship of tendon and reconstituted collagen networks [44,67,68]. We also consider three other CLs, Figs. 1(a)–1(c). These CLs all exhibit buckling-induced fiber softening and several distinct tensile responses described by a power law  $k \propto \tau^x$ :  $x = 0$  (LIN) corresponds to linear nonstiffening springs,  $x = 1/2$  (QUAD) to a quadratic force-extension relation, and  $x = 3/2$  (WLC) describes a divergent entropic force-extension relation of the worm-like chain model [36,47]. Throughout this article, we use the mechanical equilibrium response to global and local loading of these model networks to study the ability of a mechanosensor at the scale of the mesh size to glean

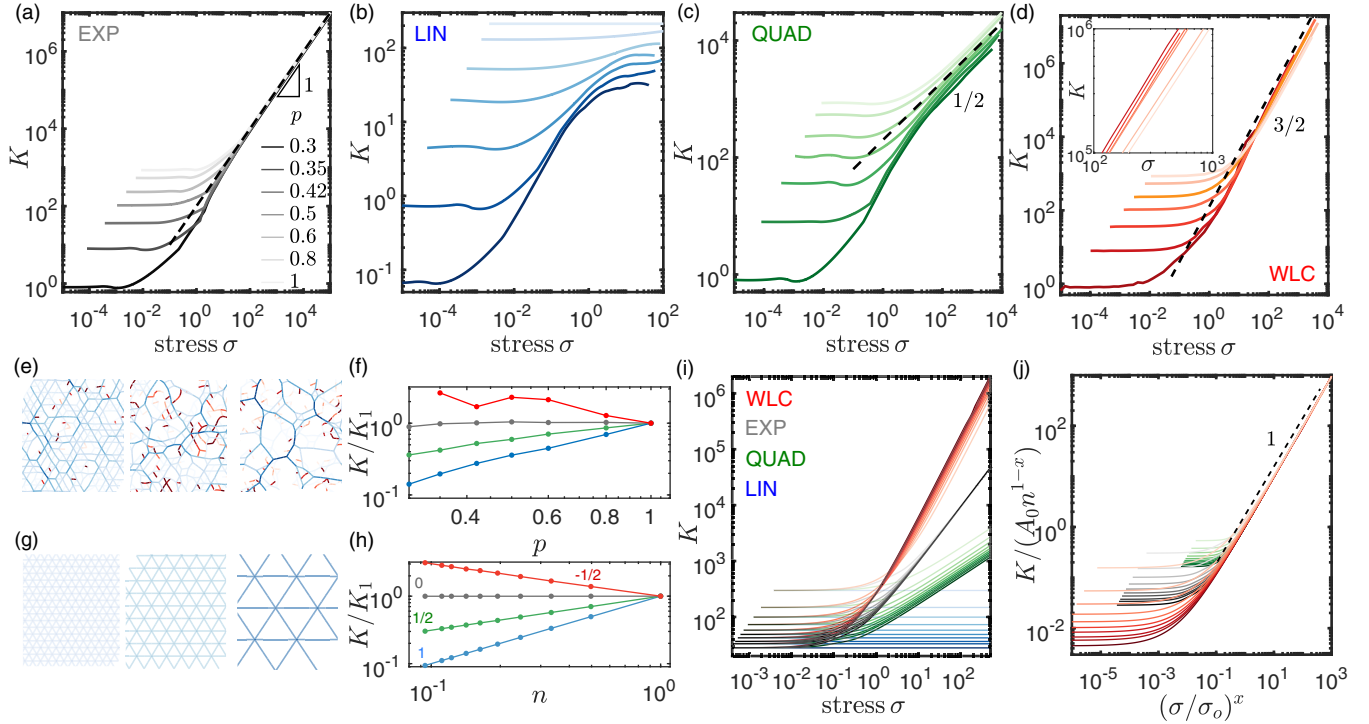


FIG. 2. Stress- and fiber density-dependence of the bulk modulus. Macroscopic differential elastic modulus ( $K$ ) vs bulk stress ( $\sigma$ ) of 3D depleted networks with various fiber densities set by the bond occupation parameter  $p$  (low to high value indicated by a dark to bright color) and constituted of (a) EXP-fibers, (b) LIN-fibers, (c) QUAD-fibers, and (d) WLC-fibers. Inset highlights the  $p$  dependence in the large-stress regime. Tension distribution in 2D EXP-fiber networks [same color code as Fig. 1(c)] of (e) randomly depleted networks with, from left to right,  $p = 0.5, 0.6,$  and  $0.8$  at a fixed stress in the asymptotic large stress regime. (f)  $p$  dependence of the large-stress modulus of 3D depleted networks. The normalization constant  $K_1$  is the modulus for the  $p = 1$  homogeneous network. (g) Same as (e) for regular networks of decreasing fiber density. (h)  $n$  dependence of the large-stress modulus of the regular networks. The normalization constant  $K_1$  is the modulus for the  $n = 1$  denser network. (i)  $K$  vs  $\sigma$  of regular networks with low to high fiber densities for the different CLs, (j) corresponding rescaled response, with  $A_0$  and  $\sigma_0$  CL-dependent constants.

information on the mechanical properties of its surrounding heterogeneous environment.

## II. DENSITY DEPENDENCE OF NONLINEAR BULK MODULUS

When using small probing forces, local measurements by a cell-scale mechanosensor are highly sensitive to density heterogeneity: the random architecture leads to some regions of the network being denser than others, thereby modulating the local mechanical properties [21–26]. To understand how, we first investigate how fiber density affects the bulk stiffness of the network. While this dependency is well understood in the linear, low-stress regime [66,69], this is not the case in the nonlinear stiffening regime arising at larger stress.

We simulate the response to a dilatation strain of networks with varying fiber density of EXP fibers representing collagen [Figs. 1(d) and 2(a)]. The network stiffness is quantified by the differential bulk modulus  $K = d\sigma/d\gamma$ , with  $\sigma$  and  $\gamma$  the macroscopic stress and strain (see Materials and Methods). At low stress, the response is linear: network stiffness is stress independent and, intuitively, increases with fiber density. In contrast, after a cross over at intermediate stresses, the modulus increases with stress as a power law  $K \propto \sigma$  that reflects the fiber constitutive nonlinearity. Strikingly, in this regime the macroscopic elastic responses *converge* to a stress-controlled

value, insensitive to fiber density, consistent with macrorheology experiments on collagen gels [44].

To elucidate the stress and density dependence of the nonlinear macroscopic response of collagen, we propose a differentially affine model. While nonaffinity, meaning local deviations from the globally applied deformation field, can be large at low stress, these nonaffine deviations decay strongly at larger stress [70]. These observations support a differentially affine model, in which increments in the deformations to additionally applied strains become slaved to the globally applied affine strain increments. Indeed, we here observe that at large stresses a tense subnetwork that carries most of the stress emerges and remains stable under further loading [Fig. 2(e), Movie S1 within the Supplemental Material (SM) [76)]. In this regime, we assume that the stress is evenly distributed among the bonds of this load-bearing subnetwork. These bonds have a density  $n$  and a tension  $\tau$ , resulting in a macroscopic stress

$$\sigma = n\tau. \quad (1)$$

In our model, we further assume that an increase  $\delta\gamma$  of the macroscopic strain results in an equal stretch  $\delta\varepsilon = \delta\gamma$  of the load-bearing fibers, i.e., that the system is differentially affine. This implies that the macroscopic differential modulus  $K$  at large stress directly reflects the microscopic differential

stiffness  $k = d\tau/d\varepsilon$  of the load-bearing fibers,

$$K = nk. \quad (2)$$

Importantly, Eqs. (1) and (2) imply strong constraints connecting the stress- and density dependence of the bulk modulus. Indeed, for fibers with power-law stiffening,  $k \propto \tau^x$ , we find at large stress that

$$K \propto \sigma^x n^{1-x}. \quad (3)$$

This equation implies that a single exponent  $x$  of the fiber-level CL controls both the  $n$  and  $\sigma$  dependence of the macroscopic modulus. Strikingly, for collagen-like fibers with  $x = 1$ , we find  $K \propto \sigma$ , independently of  $n$ . Our simple differentially affine model thus recapitulates the observations for collagen at large stress. While an alternate explanation involving normal stresses was previously proposed under shear [44], our model proposes a simple and general rationalization of the density independence of the nonlinear elastic modulus of collagen.

Our differentially affine model [Eq. (3)] also makes predictions for other CLs. For linear elements ( $x = 0$ ), we recover a stress-independent modulus proportional to  $n$ . For  $0 < x < 1$ ,  $K(\sigma)$  increases with the load-bearing bond density. Remarkably, if  $x > 1$ , we predict that  $K(\sigma)$  decreases with  $n$ . This startling behavior can be understood by considering the loading of a set of two bonds in parallel. If one of these segments is cut, the load is transferred to the remaining bond, doubling its load. If  $x = 1$ , however, this would also double the bond stiffness, thus leaving the rigidity of the system unchanged. For  $x < 1$ , depleting the network leads to a reduced modulus. By contrast, if  $x > 1$  the stiffness of the remaining bond more than doubles, clarifying our counterintuitive prediction that at constant stress, network depletion leads to stiffening.

We further confirm these predictions by simulating the fiber density- and stress-dependence of  $K$  for networks with various fiber CLs [Fig. 1]. Considering first the simple case of regular networks of variable mesh size [Fig. 2(g)], where all fibers are load bearing, we recover precisely the scaling behavior predicted by Eq. (3) [Figs. 2(h)–2(j)] and, in particular, the  $n$  dependence of the large-stress modulus [Fig. 2(h)]. For networks with random depletion [Fig. 2(e)], the fiber density is controlled by the depletion parameter  $p$ , and the connection with the load-bearing fiber density  $n$  is less evident. Qualitatively, however, we observe that the influence of  $p$  is consistent with our prediction [Fig. 2(f)]. For all four CLs considered here, our model adequately captures the stress scaling of the differential modulus  $K \propto \sigma^x$  [Figs. 2(a)–2(d)].

The scaling of  $K$  we observe can be compared with macrorheology experiments that report a stiffening exponent  $3/2$  for F-actin [47], fibrin [49], vimentin, and neurofilaments networks [48] and biomimetic hydrogels [50], whereas  $\text{Zn}^{2+}$ -modified fibrin networks exhibit an exponent  $1/2$  [71]. Our minimal model adequately captures the density dependencies observed for the different stiffening exponents [Fig. 2(h)]. In particular, for  $x > 1$ , as for WLC fibers, the differential modulus decreases for denser networks [Figs. 2(d) and 2(f)], in agreement with earlier experiments [47]. By contrast, for  $0 \leq x < 1$  denser networks display an increased modulus [Figs. 2(c) and 2(f)], as for the  $\text{Zn}^{2+}$ -modified fibrin networks [71]. Taken together, our results show how at large

stress the fiber density controls the mechanical response of soft heterogeneous networks in a way that depends sensitively on the nonlinear micromechanics of the constituents. Interestingly, collagen networks stand out by uniquely displaying a stress-controlled mechanical response independently of network fiber density.

### III. LARGE FORCE ENSURES ROBUST LOCAL RESPONSE

To determine the macroscopic mechanical information a cell can in principle obtain by performing local mechanical measurements inside a disordered network, we consider the mechanical measurements performed by an ideal mechanosensor. Such an ideal mechanosensor probes the network by actively exerting a force at the scale of the network mesh size and measures the network's local compliance without error. To conceptually understand how such a mechanosensor probes its mechanical microenvironment in the simplest possible setting, we study the response of fiber networks to point-like force monopoles.

We employ the model introduced in Fig. 1 and simulate local loading induced by a point-force monopole in a large spherical network with fixed boundary conditions [Fig. 3(c) inset; see Materials and Methods]. This setup is informative for mechanosensing as it allows us not only to probe the network at the cellular scale, but also to apply forces that are large enough to locally trigger the nonlinear response of a matrix, as observed in the vicinity of cells embedded in fibrous matrices [33–35]. Numerically, to avoid boundary effects and correlations between individual measurements considered in [22], we perform a local mechanical probe in the center of independently sampled network configurations.

For collagen-like fibers with EXP CL, we measure many statistically independent force-displacement curves [Fig. 3(a)]. These responses reveal two key features: (i) the curves exhibit large variability, with a broad distribution of displacements at any force level, and (ii) they are nonlinear and exhibit a pronounced stiffening response. For each force-displacement curve  $F(u)$  we measure locally, we determine the differential stiffness  $k = dF/du$  as a function of force [Fig. 3(b)]. Indeed, while it has been suggested that cells could be sensitive to several quantities such as the strain energy [72], viscoelastic properties [73], and stiffness with extensive evidence [12–15, 35, 74, 75], a complete determination of the mechanical variables cells respond to is still lacking, especially in nonlinear environments. However, as cells have been shown to adapt to the stiffness in collagen matrices, including the local differential stiffness increased by the forces exerted by the cell [35], we here characterize the mechanical response of a cell-scale mechanosensor in terms of this differential mechanical quantity.

At low forces ( $F < 1$ ),  $k$  is independent of  $F$  and this linear response is highly heterogeneous. Thus, at low forces a cell-scale mechanosensor can only acquire unreliable information about the mechanical landscape of their environment, as previously observed [21–25]. As the force is increased, however, the network stiffens, with locally softer networks stiffening at lower probe forces. Remarkably, at large forces ( $F \geq 10$ ), the stiffness no longer strongly varies relative to

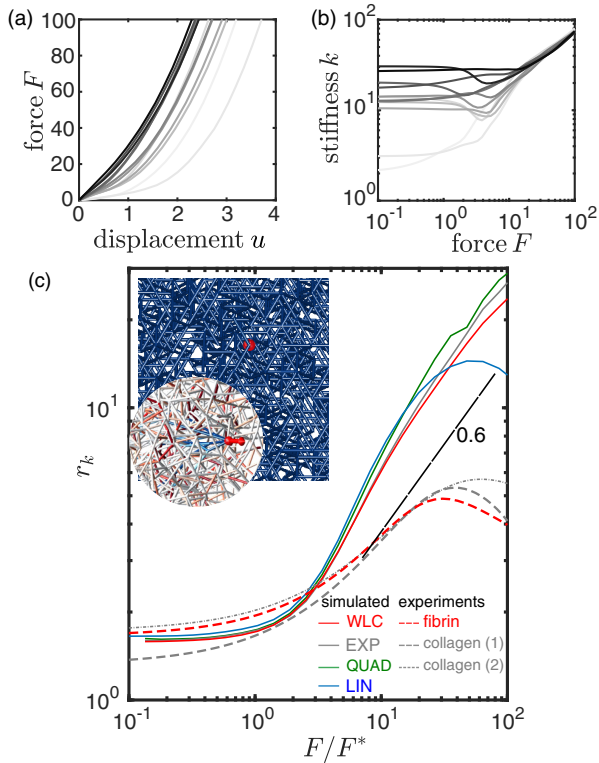


FIG. 3. Nonlinear response to local probing of an ideal mechanosensor in disordered fibrous networks. Local probing of 3D depleted EXP-fibers networks, small random sample of measurements performed, (a) applied force ( $F$ ) vs measured displacement ( $u$ ) of the monopoles embedded at various locations, (b) corresponding differential stiffness ( $k$ ) vs  $F$ . (c) Signal-to-noise ratio ( $r_k$ ) of the stiffness measurements vs applied force, normalized by the force  $F^*$  at the onset of the power law regime, for simulated networks with different CLs [Fig. 1] and microrheology measurements on two collagen and one fibrin gels. Rectangular inset: a probe (red sphere) in the center of a numerically generated disordered network; circular inset: tension distribution in fibers located behind the probe [ $F = 10$ , same colorcode as in Fig. 1(d)].

the mean [Fig. 3(b)]. This transition from a highly fluctuating differential stiffness in the linear response regime, where soft bending deformations dominate the response [22], to a large force regime where measurements converge towards a single  $k(F)$  curve, is consistent with the behavior observed with microrheology measurements in collagen networks [33]. Thus, in this nonlinear regime, the local mechanical properties that a cell-scale mechanosensor could measure inside a fibrous matrix becomes reliable and increasingly robust to local fluctuations in fiber density, as observed for cells in collagen [33,35].

This may appear unsurprising in light of the fiber density independence of the nonlinear macroscopic modulus of a collagen network at fixed stress [44] [Fig. 2(a), Eq. (3)]. However, to show that the observed macroscopic density independence of collagen networks does not explain the convergence of the microscopic  $k(F)$  curves, which become independent of local fiber density heterogeneity, we perform microrheological simulations on networks with other fiber CLs [Figs. 1(a)–1(c)] whose nonlinear bulk stiffness is *not*

independent of average fiber density. Surprisingly, we observe the same features for all CLs (Fig. S5 within the SM [76]): the local stiffness strongly fluctuates in the linear response regime, while the various differential measurements robustly tend to a single master curve at large forces.

To further quantify this increased robustness, we characterize the ensemble of independent stiffness values at a given force in terms of the signal-to-noise ratio  $r_k = \langle k \rangle / \text{std}(k)$  [Fig. 3(c)]. This ratio quantifies how well a particular mechanical measurement inside a disordered medium compares to the average mechanical properties. As  $r_k$  increases with force, the mechanical signal becomes stronger relative to the mechanical heterogeneity. Interestingly, we find that the growth of  $r_k$  with increasing force can be approximated as a power law in the nonlinear regime,

$$r_k = \frac{\langle k \rangle}{\text{std}(k)} \sim F^\alpha. \quad (4)$$

We measure  $\alpha \approx 0.6$  for our simulated mechanical responses. This exponent is also independent of network dimensionality (Fig. S1 within the SM [76]). In addition,  $\alpha$  does not vary substantially when changing the CL: convergence of measurements is observed in all cases according to this universal power law.

To experimentally test our prediction of the constituent-independent exponent  $\alpha$  describing the increased robustness of local mechanosensation, we follow the microrheology experiments described in [33] and expand by probing biopolymers with distinct nonlinear bulk properties [44,77]: reconstituted collagen and fibrin networks (Fig. S9 within the SM [76], see Materials and Methods). Indeed, for both matrices we observe a marked increase of  $r_k$  in the nonlinear response regime. The observed discrepancies, in particular the narrow force range over which the power law is observed, can have several possible origins such as finite size effects, a limited control of the particle location with respect to the boundary and fluctuations in terms of particle radius vs pore size. Nevertheless, we observe a marked increase similar to that observed in simulations [Fig. 3(c)]. Therefore, the origins of this microrheological robustness cannot be the same as for the macrorheological convergence of nonlinear bulk modulus, which is specific to collagen.

In summary, at low force a single mechanical measurement is a poor estimator of the network's average mechanical properties: Mechanosensing is strongly limited by structural heterogeneities. By contrast, our experiments and simulations indicate that the local mechanical response of fiber networks becomes largely insensitive to structural disorder at large force.

#### IV. NONLINEAR MECHANOSENSING MODEL

As the increased robustness of local micromechanical measurements at large force is generically observed for a range of CLs, we argue that its physical origin must lie in the fibrous structure of the network, rather than in the specific micromechanical properties of its constituents. This is further supported by the modest influence of the CL on differential stiffness in the nonlinear regime: While at the macroscopic scale the bulk modulus followed  $K \sim \sigma^x$  at large stress, the

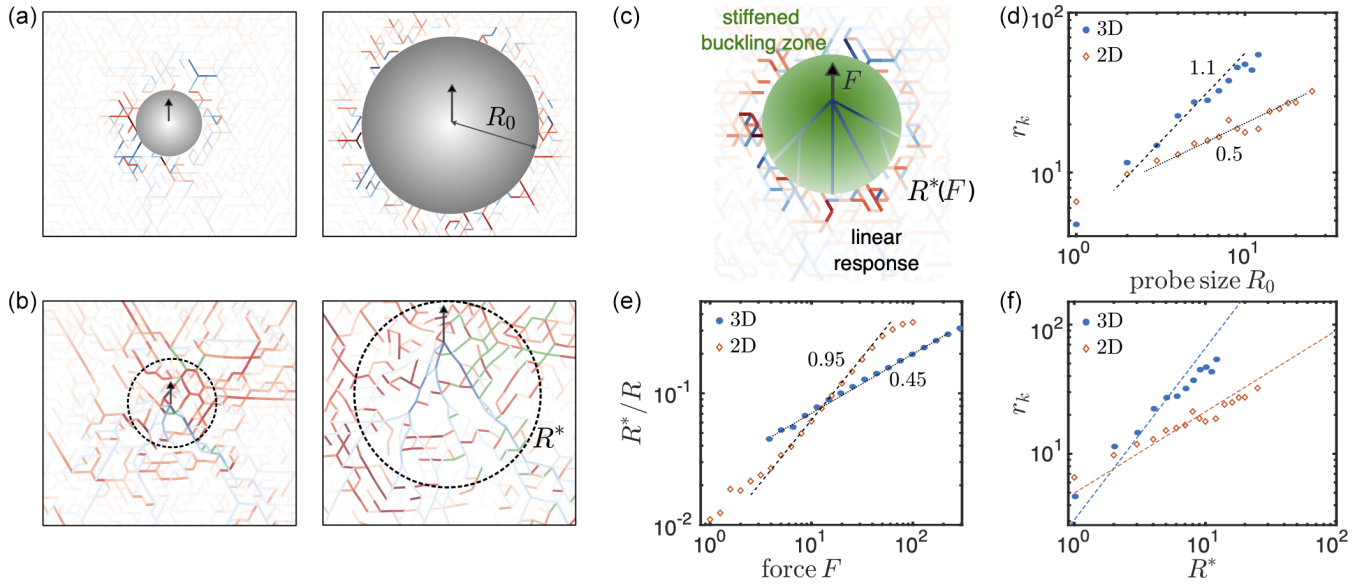


FIG. 4. Scale-dependent nonlinear mechanosensation. Local probing of depleted EXP-fibers networks. (a) Tension distribution in 2D networks loaded by probes (gray circular objects) of two different radius  $R_0$  [ $F = 0.001$ , same tensions color code as in Fig. 1(d)]. (b) Highlight of the nonlinear region  $R^*$  (dashed circle) surrounding the point-force probe (arrow). The buckled fibers are shown in green (only on the right half of the figure). (c) Schematics of the stiffened buckling zone embedded in a linearly deforming soft network. (d) Signal-to-noise ratio ( $r_k$ ) of stiffness measurements as a function of the probe radius ( $R_0$ ) for an applied probe force  $F = 0.001$ . (e) Radius of the buckling region  $R^*$ , normalized by the system radius  $R$ , vs  $F$  applied by a point-force probe. (f) Comparison of the measured (dots and diamonds) and expected (dashed lines) signal-to-noise ratio, determined using Eqs. (4) and (6), as a function the size of the probe taken as  $R^*$ .

exponent  $x$  does not set the microscopic stiffening response [78] (Fig. S5G within the SM [76]). Building on recent theoretical results showing that the nonlinear response of fiber networks to force dipoles results in an effective increase of the dipole size [62], we propose that this robustness can instead be understood in terms of an effective increase of the size of the probed region. As network heterogeneity averages out on larger scales, this would imply that, as the force increases, the probe becomes less sensitive to local density fluctuations.

To explore this idea, we first examine the linear local response and investigate how the size of the mechanosensory probe affects relative stiffness fluctuations of both 2D and 3D networks with EXP fibers. While a measurement integrates mechanical contributions at all scales, the rapid decay of linear elastic deformations [79] leads to a dominant contribution of density fluctuations in a small volume in the vicinity of the probe [22]. Consequently, individual measurements strongly depend on their location and the corresponding stiffness values display a large variability. A larger probe, however, samples the local mechanics of a bigger region in the vicinity of the network, thereby averaging more effectively over structural heterogeneity. Larger probes are thus more informative about the system's macroscopic response.

To demonstrate that increasing probe size indeed leads to more robust measurements, we perform simulations of a circular rigid body of radius  $R_0$  applying a small force monopole ( $F = 0.001$ ) to the network [Fig. 4(a)]. For each probe radius  $R_0$ , we compute the signal-to-noise ratio of linear stiffnesses, revealing a power-law increase

$$r_k \sim R_0^\beta \quad (5)$$

with  $\beta \simeq 0.5$  in 2D and  $\beta \simeq 1.1$  in 3D [Fig. 4(d)]. This power law increase of  $r_k$  with probe size confirms that the responses depend less on local fiber density fluctuations.

We tentatively connect this increased robustness of local sensing of the linear mechanical response with probe size to the increased robustness we observe in the nonlinear response for large local probing forces [Fig. 3(c)]. Thus, we argue that a sufficiently large applied force triggers the response of the network over an effectively larger region than in the linear response regime. To determine the force-dependent length-scale that sets the local response, we note that at the onset of the nonlinear response, fibers start to buckle near the probe [Fig. 4(b) left]. Buckling spreads to a larger region in the network as the applied force increases [62] [Fig. 4(b) right]. This leads to the emergence of a “buckling zone” of growing size  $R^*$  with both a large density of buckled fibers that lifts orthoradial constraints and the formation of tensed rope-like structures in the radial direction. These load-bearing fibers display enhanced alignment and contribute to the stiffening [43,64]. Consequently, within the buckling zone the network strain stiffens in the radial direction as the elastic response is dominated by stretching of the ropes, which is a much stiffer mode of deformation than the fiber bending modes governing the linear response regime [38]. As buckling and other geometric nonlinearities are inevitable and necessarily introduce an asymmetric response that is inherent to fiber networks, this emergence of this strain stiffening region does not rely on the particular CL we employ.

A probe force deforms both the network inside the buckling zone and the surrounding network beyond  $R^*$ . These two network sections thus effectively act as two mechanical elements in series. Because the buckling zone strain stiffens, however,

it becomes much stiffer than the network section beyond  $R^*$  that is still dominated by soft bending modes [Fig. 4(c)]. To first approximation, the buckling zone therefore becomes effectively rigid, and the compliance in response to the probe is dominated by the linear response of the network beyond  $R^*$ . Thus, elastic nonlinearity renders the network disorder irrelevant inside the stiffened buckling zone, and local stiffness fluctuations are instead determined by network disorder outside the nonlinear zone. Put simply, the emergent length scale  $R^*$  renormalizes the size of the local probe in a force-dependent way. Local probes with large enough forces thus effectively probe the local linear mechanical properties of the network over a larger length scale making the response less sensitive to local disorder.

To understand the force dependence of the buckling zone radius induced by monopole probing, we perform an analysis similar to previous studies on dipole-induced buckling [60,62,63]. Away from the probe, the stress decays as  $\sigma(r) \sim F/r^{D-1}$  due to force conservation. From the buckling condition, here written in terms of stress as  $\sigma \sim \sigma_b$ , with  $\sigma_b$  the buckling stress, we expect  $\sigma(R^*) \sim \sigma_b$ . Therefore, buckling occurs over a region of size

$$R^* \sim F^\zeta \quad (6)$$

with  $\zeta = 1/(D - 1)$ . Indeed, we measure  $\zeta \simeq 0.45$  in 3D and 0.95 in 2D in our simulations (Fig. 4(e), Figs. S7 and S8 within the SM [76]).

To complete our nonlinear mechanosensing model, we now quantitatively connect the increase of  $r_k$  with probe size in the linear response regime [Eq. (5)] to the power-law increase of  $r_k$  with the applied point force [Eq. (4)]. To do so, we identify the effective probe size  $R_0$  induced by nonlinear effects with the buckling length-scale  $R^*$ . Using Eqs. (4) and (6), our nonlinear mechanosensing model predicts a power-law increase of  $r_k$  with the buckling range  $R^*$ :  $r_k \sim R^{*\alpha/\zeta}$ . Importantly, for both 2D and 3D simulated responses the expected power-law increase is consistent with Eq. (5) (Fig. 4(f), Table 1 within the SM [76]). Thus, our scaling model establishes that locally probing the network in the nonlinear regime can be conceptualized as a linear probe with a renormalized probing radius associated to the radius of the buckling zone. This model quantitatively explains the CL-independent increase of mechanosensation reliability at large forces in fiber networks.

## V. NONLINEAR MECHANOSENSATION IS RELIABLE

Could a nonlinear mechanosensor reliably infer the large-scale mechanical properties of their surrounding matrix from local stiffness measurements? Two ingredients are needed for reliable mechanosensation: the local measurements should have low noise, but importantly they should also be informative about the macroscopic stiffness. To address this question, we consider local mechanical measurements performed in EXP-fibers networks with varying mean fiber density [Fig. 5(a)], which sensitively tunes the linear macroscopic modulus  $K_0$  [44,47–50,66,69,71].

We find that in the low-force regime, there is a large overlap of the local differential stiffness measurements in networks with different  $p$  values: the variation of individual measurements exceeds the difference in mean stiffness of networks

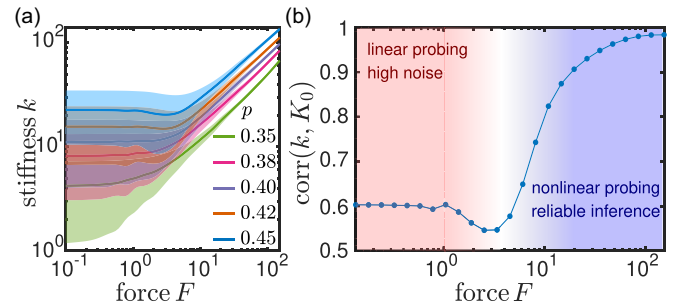


FIG. 5. Robust nonlinear mechanosensing. (a) Mean stiffness as a function of force for different values of  $p$ , the shaded areas show the stiffness standard deviation. (b) Pearson correlation coefficient between the local stiffness ( $k$ ) and the linear bulk modulus ( $K_0$ ) as a function of the local probing force.

with different fiber densities. More quantitatively, we find that individual local stiffness measurements are only weakly correlated with  $K_0$  in the linear regime, as quantified by the Pearson’s correlation coefficient [Fig. 5(b)]. Mechanosensation based on such linear stiffness measurements is thus highly unreliable.

By contrast, at large forces the differential stiffness measured on networks with different fiber densities become clearly separated [Fig. 5(a)] and these local nonlinear measurements strongly correlate with the bulk stiffness [Fig. 5(b)]. The Pearson correlation coefficient approaches 1 at large forces: A single nonlinear local stiffness measurement is thus sufficiently informative to accurately infer bulk network properties. By probing the mechanical response with large force, a cell could thus in principle robustly measure the average nonlinear mechanical properties of its surroundings and discriminate between the materials properties of networks of varying fiber density.

## VI. DISCUSSION

To understand the physical limits of nonlinear mechanosensing, we studied the response of disordered networks to local force probes at the cell scale. Using a fiber network model, we demonstrated that a local ideal mechanosensor can reliably determine both the local and macroscopic mechanical response of the disordered network by triggering elastic nonlinearities. This nonlinear mechanosensation becomes progressively insensitive to network disorder with increasing force, as confirmed via microrheology experiments. Nonlinear mechanosensing thus offers cells a reliable strategy to both locally determine and control the mechanical properties of a disordered ECM.

We showed that macroscopic and microscopic nonlinear responses of disordered fiber networks are set by distinct mechanisms arising because nonlinearities affect the mechanical response in a different way at the two scales. Macroscopically, the network stiffens approximately homogeneously and the differential bulk stiffness is a power law of the applied stress in the nonlinear regime [Figs. 2(a)–2(d)], with an exponent  $x$  set by the constitutive stiffening of a single fiber [Fig. 1(c)]. We capture this macroscopic behavior with a differentially affine model. This model predicts that the

load-bearing fiber density dependence of the differential bulk modulus is set by an exponent  $1 - x$  [Eq. (3)], which thus solely depends on the constitutive fiber stiffening [Fig. 2(h)]. Remarkably, this implies that the differential modulus of collagen ( $x = 1$ ) uniquely becomes insensitive to fiber density at large stress [Fig. 2(a)], as observed experimentally [44]. Our model further offers insights into experiments with different stress and density dependencies on various reconstituted networks with distinct stiffening behaviors [44,47–50,71]. Microscopically, in contrast, the network stiffens heterogeneously and the local differential stiffness also increases with force as a power-law (Fig. S5 within the SM [76]), but with an exponent that is not determined by the constitutive fiber stiffening [78]. Instead, this local stiffening is controlled by force-induced buckling and network nonlinearity in the form of a bending-stretching stiffening transition, giving rise to a stiffened buckling zone embedded in a linearly responding network [Fig. 4(c)]. Thus, local force stiffening is caused by the effective probing of the linear network stiffness at increasingly larger scales set by the buckling zone radius. The linearly deforming network at these larger scales sets the mechanical response, which hence remains density dependent. Our results on the difference between microscopic and macroscopic stiffening mechanisms could be used to further develop accurate approaches for 3D traction force inference or stress inference around cells in 3D matrices [33,35].

The emergence of the stiffened buckling zone explains the mechanical robustness to local force probes. Indeed, a sufficiently large force effectively probes the linear response averaged over the structural disorder of an enlarged region of the network, with dimension set by the force-dependent buckling length-scale. This elastic regime is relevant for cell-ECM mechanical interactions. Indeed, several cell types apply traction forces of the order of tens of nanonewtons [29–32,80]. These forces can trigger the nonlinear response of reconstituted networks, as shown by our microrheology measurements in collagen and fibrin (Fig. S9 within the SM [76]). This nonlinear response is consistent with observations of contractile cells in a matrix: Fibers buckle [33] and displacements are enhanced, decreasing more slowly than predicted by linear elasticity [35,61,81]. Furthermore, the network stiffens in the wake of a cell applying traction [33,35,81], and our nonlinear mechanosensing model can be used to determine the stiffness such cells could locally determine and respond to. The magnitude of the force cells need to exert on their substrate to employ nonlinear mechanosensation *in vivo* likely depends on context, where softer environments typically require smaller forces to trigger nonlinearity. Thus, even though neurons apply smaller forces [82] than, e.g., fibroblasts or cardiomyocytes [80], differences in stiffness and nonlinear force thresholds of the natural surroundings could still allow such different cells to employ nonlinear mechanosensation.

The formation of the force-controlled buckling zone is qualitatively independent of the local structure of the probe forces. In particular, the characteristic length-scale emerging in response to dipole loading is well characterized [62–64]. We thus expect a similar robustness increase as a power law for dipole mechanosensors, but with modified exponents. Since cells are mechanically better described as force dipoles [83], this anticipated power-law increase in response to dipole

loading further supports nonlinear mechanosensing as a cellular strategy.

Many aspects of cellular mechanosensation are still debated, including the internal cellular machinery and processes that are involved, as well as the mechanical variable that can be sensed by cells [84,85]. Here, we characterized the reliability of the mechanical response in terms of stiffness, a mechanical property that is experimentally shown to influence cellular behavior [12–15,35,74,75]. Yet, cells are also found to respond to other mechanical variables, such as the substrate strain energy [72]. Therefore, one could consider other mechanical quantities to assess the limits of nonlinear mechanosensing, such as strain and elastic energies, which we characterized as alternatives (Fig. S6 within the SM [76]). In these cases, the signal-to-noise ratio also generically increase with force for networks with a range of fiber constituents. This is understandable since local sensing becomes nonlocal due to the emergence of the buckling zone that facilitates disorder averaging over an increased length scale, regardless of the precise mechanical variable that is considered. Therefore, we argue that enhanced nonlinear mechanosensing is a general characteristic of disordered fibrous networks.

Finally, our paper suggests that cells could employ nonlinear mechanosensation as a strategy to reliably sense and respond to the stiffness of their environment. In the linear regime, cells face a highly heterogeneous mechanical landscape [21–25]. If this linear regime dominated cell-ECM interactions, we would expect the mechanical heterogeneity perceived by cells to lead to erratic stiffness-dependent cell behaviors following the large local stiffness fluctuations in the ECM. In contrast, if cells trigger the nonlinear response with large forces, then our nonlinear mechanosensation model implies that cells instead face a strikingly homogeneous mechanical landscape that is directly correlated with the matrix macroscopic modulus, and where stiffness-dependent cell behavior would become coherent and would no longer depend randomly on the cell's location in the matrix. Nonlinear mechanosensation also has implications for the cell's ability to control the stiffness of their environment. The idea that cells actively stiffen their matrix and adapt in response to the enhanced stiffness has long been introduced [35,77,81], and it was speculated that such a feedback mechanism aims at reaching a specific substrate resistance. We here propose that nonlinear mechanosensation allows cells to exploit this mechanical feedback to accurately control their surrounding stiffness despite the inherent randomness of their local environment, allowing them to robustly perform mechanosensitive cellular functions even in a highly disordered ECM.

## VII. MATERIALS AND METHODS

### A. Random network generation

Networks are generated by placing straight fibers on an ordered triangular (2D) or face centered cubic (3D) lattice. These networks are randomly depleted with a bond occupation probability  $p$ . Unless stated otherwise, we use  $p = 0.6$  in 2D and  $p = 0.4$  in 3D.

### B. Mechanical model

Fibers are discretized with bonds of rest length  $\ell_0 = 1$ . Each bond acts as a spring with linear stretching modulus

$\mu = 100$  and their nonlinear longitudinal response  $f(\epsilon_{ij})$  is described by a CL displayed in Fig. 1. Fibers also resist transverse deflection with a bending rigidity  $\kappa = 1$  that penalizes deflections of angle  $\theta$ . Fibers are connected by freely deforming hinges at their intersection. We consider a probe located on sites  $i$  of position  $\mathbf{R}_i$  and applying a force  $\mathbf{F}_i$ . The Hamiltonian of the system is

$$\mathcal{H} = - \sum_{\text{forces } i} \mathbf{F}_i \cdot \mathbf{R}_i + \sum_{\text{bonds } (i,j)} f(\epsilon_{ij}) + \sum_{\text{hinges } (i,j,k)} 2 \sin^2 \frac{\theta_{ijk}}{2}.$$

### C. Macroscopic loading

The boundaries of the network are displaced to impose isotropic dilatation. Our depleted networks have dimensions  $30 \times 30 \times 30$  and periodic boundary conditions are imposed. The results are averaged over three independent random networks. The bulk stress and bulk modulus are computed from the first and second derivative of the system's energy,

$$\sigma = \frac{1}{V} \frac{\partial \mathcal{H}}{\partial \gamma}, \quad K = \frac{1}{V} \frac{\partial^2 \mathcal{H}}{\partial \gamma^2}$$

where  $\gamma$  is the applied dilatation strain and  $V$  the system's volume.

### D. Local probing

A point force  $F$  is applied to a vertex at the center of spherical (circular in 2D) depleted networks of radius  $R = 40$  in 3D ( $R = 100$  in 2D) for QUAD-, EXP- and WLC fibers, and  $R = 45$  for LIN fibers. Finite-size effects on the stiffness statistics are displayed in Fig. S3 within the SM [76]. The probe loading direction is  $[0,1,0]$ , not following any fiber direction in the undeformed network. The network boundaries are fixed. For each CL, 100 disorder realizations are performed. To determine  $r_k$  vs  $R_0$  [Fig. 4(d)], the same boundary conditions apply and a sphere (disk) of radius  $R_0$  is placed in the system's center ( $R = 30$  in 3D, refer to Fig. S4 within the SM [76] for a characterization of finite size effects and  $R = 200$  in 2D) All bonds within the probe are removed and

we apply a force  $F = 10^{-3}$  in the direction  $[0,1,0]$  to all intersecting nodes, which move collectively as one rigid body. One hundred network realizations are used.

### E. Numerical resolution

At each applied loading, mechanical equilibrium is obtained by minimizing the total energy using the GNU Scientific Library BFGS implementation of the Broyden-Fletcher-Goldfarb-Shanno algorithm.

### F. Microrheology experiments

Experimental and data analysis procedures are performed as described in [33] and [78]. Briefly, microparticles ( $2 \mu\text{m}$  in diameter, C37278, ThermoFisher) are embedded in  $4 \text{ mg/mL}$  collagen gel and  $3 \text{ mg/mL}$  fibrin gel. A homemade optical tweezer is used to drag the particle at a velocity of  $1 \mu\text{m/s}$ . The displacements of the particles and the optical forces are recorded.

Data used in this article have been deposited on Zenodo [86].

### ACKNOWLEDGEMENTS

This project has received funding (E.B. and C.P.B.) from the European Union's Horizon 2020 research and innovation programme under the Marie Skłodowska-Curie Grant Agreement No. 891217 and the Deutsche Forschungsgemeinschaft (DFG, German Research Foundation)-Project ID 201269156-SFB 1032 (Project B12). P.R. is supported by France 2030, the French National Research Agency (ANR-16-CONV-0001) and the Excellence Initiative of Aix-Marseille University-A\*MIDEX. M.G. and H.Y. acknowledge support from NIH Grant No. 1R01G140108. E.B., C.B., and P.R. would like to acknowledge, in order of appearance, Jesse, Milou, Arielle, Lise, Ella and H el ene, for being wonderful reasons of this work's publication delay.

The authors have no competing interests to declare.

- 
- [1] A. Shellard and R. Mayor, All roads lead to directional cell migration, *Trends Cell Biol.* **30**, 852 (2020).
  - [2] M. A. Wozniak and C. S. Chen, Mechanotransduction in development: A growing role for contractility, *Nat. Rev. Mol. Cell Biol.* **10**, 34 (2009).
  - [3] C.-P. Heisenberg and Y. Bella iche, Forces in tissue morphogenesis and patterning, *Cell* **153**, 948 (2013).
  - [4] O. Camp s, T. Mammoto, S. Hasso, R. A. Sperling, D. O'connell, A. G. Bischof, R. Maas, D. A. Weitz, L. Mahadevan, and D. E. Ingber, Quantifying cell-generated mechanical forces within living embryonic tissues, *Nat. Methods* **11**, 183 (2014).
  - [5] P. A. Janmey and R. T. Miller, Mechanisms of mechanical signaling in development and disease, *J. Cell Sci.* **124**, 9 (2011).
  - [6] D. Wirtz, K. Konstantopoulos, and P. C. Searson, The physics of cancer: The role of physical interactions and mechanical forces in metastasis, *Nat. Rev. Cancer* **11**, 512 (2011).
  - [7] D. E. Discher, P. Janmey, and Y.-L. Wang, Tissue cells feel and respond to the stiffness of their substrate, *Science* **310**, 1139 (2005).
  - [8] V. Vogel and M. Sheetz, Local force and geometry sensing regulate cell functions, *Nat. Rev. Mol. Cell Biol.* **7**, 265 (2006).
  - [9] A. D. Doyle and K. M. Yamada, Mechanosensing via cell-matrix adhesions in 3D microenvironments, *Exp. Cell Res.* **343**, 60 (2016).
  - [10] D. E. Minner, P. Rauch, J. K as, and C. A. Naumann, Polymer-tethered lipid multi-bilayers: A biomembrane-mimicking cell substrate to probe cellular mechano-sensing, *Soft Matter* **10**, 1189 (2014).
  - [11] D. E. Koser, A. J. Thompson, S. K. Foster, A. Dwivedy, E. K. Pillai, G. K. Sheridan, H. Svoboda, M. Viana, L. da F Costa, J. Guck *et al.*, Mechanosensing is critical for axon growth in the developing brain, *Nat. Neurosci.* **19**, 1592 (2016).
  - [12] A. J. Engler, S. Sen, H. L. Sweeney, and D. E. Discher, Matrix elasticity directs stem cell lineage specification, *Cell* **126**, 677 (2006).
  - [13] F. Chowdhury, S. Na, D. Li, Y.-C. Poh, T. S. Tanaka, F. Wang, and N. Wang, Material properties of the cell dictate stress-induced spreading and differentiation in embryonic stem cells, *Nat. Mater.* **9**, 82 (2010).

- [14] C.-M. Lo, H.-B. Wang, M. Dembo, and Y.-L. Wang, Cell movement is guided by the rigidity of the substrate, *Biophys. J.* **79**, 144 (2000).
- [15] A. Shellard and R. Mayor, Durotaxis: The hard path from *in vitro* to *in vivo*, *Dev. Cell* **56**, 227 (2021).
- [16] M. Dietrich, H. Le Roy, D. B. Brückner, H. Engelke, R. Zantl, J. O. Rädler, and C. P. Broedersz, Guiding 3D cell migration in deformed synthetic hydrogel microstructures, *Soft Matter* **14**, 2816 (2018).
- [17] P. A. Janmey, D. A. Fletcher, and C. A. Reinhart-King, Stiffness sensing by cells, *Physiol. Rev.* **100**, 695 (2020).
- [18] Q. Wen and P. A. Janmey, Effects of non-linearity on cell-ECM interactions, *Exp. Cell Res.* **319**, 2481 (2013).
- [19] N. R. Lang, S. Münster, C. Metzner, P. Krauss, S. Schürmann, J. Lange, K. E. Aifantis, O. Friedrich, and B. Fabry, Estimating the 3d pore size distribution of biopolymer networks from directionally biased data, *Biophys. J.* **105**, 1967 (2013).
- [20] C. Frantz, K. M. Stewart, and V. M. Weaver, The extracellular matrix at a glance, *J. Cell Sci.* **123**, 4195 (2010).
- [21] M. J. Grill, J. Kernes, V. M. Slepukhin, W. A. Wall, and A. J. Levine, Directed force propagation in semiflexible networks, *Soft Matter* **17**, 10223 (2021).
- [22] F. Beroz, L. M. Jawerth, S. Münster, D. A. Weitz, C. P. Broedersz, and N. S. Wingreen, Physical limits to biomechanical sensing in disordered fibre networks, *Nat. Commun.* **8**, 16096 (2017).
- [23] M. Proestaki, A. Ogren, B. Burkel, and J. Notbohm, Modulus of fibrous collagen at the length scale of a cell, *Exp. Mech.* **59**, 1323 (2019).
- [24] C. A. Jones, M. Cibula, J. Feng, E. A. Krnacik, D. H. McIntyre, H. Levine, and B. Sun, Micromechanics of cellularized biopolymer networks, *Proc. Natl. Acad. Sci. USA* **112**, 5117 (2015).
- [25] A. Hayn, T. Fischer, and C. T. Mierke, Inhomogeneities in 3d collagen matrices impact matrix mechanics and cancer cell migration, *Front. Cell Dev. Biol.* **8**, 593879 (2020).
- [26] M. Proestaki, B. Burkel, E. E. Galles, S. M. Ponik, and J. Notbohm, Effect of matrix heterogeneity on cell mechanosensing, *Soft Matter* **17**, 10263 (2021).
- [27] F. Serwane, A. Mongera, P. Rowghanian, D. A. Kealhofer, A. A. Lucio, Z. M. Hockenbery, and O. Campas, *In vivo* quantification of spatially varying mechanical properties in developing tissues, *Nat. Methods* **14**, 181 (2017).
- [28] A. Mongera, M. Pochitaloff, H. J. Gustafson, G. A. Stooke-Vaughan, P. Rowghanian, S. Kim, and O. Campàs, Mechanics of the cellular microenvironment as probed by cells *in vivo* during zebrafish presomitic mesoderm differentiation, *Nat. Mater.* **22**, 135 (2023).
- [29] L. Trichet, J. Le Digabel, R. J. Hawkins, S. R. K. Vedula, M. Gupta, C. Ribault, P. Hersen, R. Voituriez, and B. Ladoux, Evidence of a large-scale mechanosensing mechanism for cellular adaptation to substrate stiffness, *Proc. Natl. Acad. Sci. USA* **109**, 6933 (2012).
- [30] T. Freyman, I. Yannas, R. Yokoo, and L. Gibson, Fibroblast contractile force is independent of the stiffness which resists the contraction, *Exp. Cell Res.* **272**, 153 (2002).
- [31] J. L. Tan, J. Tien, D. M. Pirone, D. S. Gray, K. Bhadriraju, and C. S. Chen, Cells lying on a bed of microneedles: An approach to isolate mechanical force, *Proc. Natl. Acad. Sci. USA* **100**, 1484 (2003).
- [32] W. R. Legant, J. S. Miller, B. L. Blakely, D. M. Cohen, G. M. Genin, and C. S. Chen, Measurement of mechanical tractions exerted by cells in three-dimensional matrices, *Nat. Methods* **7**, 969 (2010).
- [33] Y. L. Han, P. Ronceray, G. Xu, A. Malandrino, R. D. Kamm, M. Lenz, C. P. Broedersz, and M. Guo, Cell contraction induces long-ranged stress stiffening in the extracellular matrix, *Proc. Natl. Acad. Sci. USA* **115**, 4075 (2018).
- [34] S. Van Helvert and P. Friedl, Strain stiffening of fibrillar collagen during individual and collective cell migration identified by AFM nanoindentation, *ACS Appl. Mater. Interfaces* **8**, 21946 (2016).
- [35] M. S. Hall, F. Alisafaei, E. Ban, X. Feng, C.-Y. Hui, V. B. Shenoy, and M. Wu, Fibrous nonlinear elasticity enables positive mechanical feedback between cells and ECMs, *Proc. Natl. Acad. Sci. USA* **113**, 14043 (2016).
- [36] F. C. MacKintosh, J. Käs, and P. A. Janmey, Elasticity of semiflexible biopolymer networks, *Phys. Rev. Lett.* **75**, 4425 (1995).
- [37] E. M. Huisman, C. Heussinger, C. Storm, and G. T. Barkema, Semiflexible filamentous composites, *Phys. Rev. Lett.* **105**, 118101 (2010).
- [38] C. P. Broedersz and F. C. MacKintosh, Modeling semiflexible polymer networks, *Rev. Mod. Phys.* **86**, 995 (2014).
- [39] C. Storm, J. J. Pastore, F. C. MacKintosh, T. C. Lubensky, and P. A. Janmey, Nonlinear elasticity in biological gels, *Nature (London)* **435**, 191 (2005).
- [40] P. R. Onck, T. Koeman, T. Van Dillen, and E. van der Giessen, Alternative explanation of stiffening in cross-linked semiflexible networks, *Phys. Rev. Lett.* **95**, 178102 (2005).
- [41] A. M. Stein, D. A. Vader, D. A. Weitz, and L. M. Sander, The micromechanics of three-dimensional collagen-I gels, *Complexity* **16**, 22 (2011).
- [42] E. Ban, H. Wang, J. M. Franklin, J. T. Liphardt, P. A. Janmey, and V. B. Shenoy, Strong triaxial coupling and anomalous poisson effect in collagen networks, *Proc. Natl. Acad. Sci. USA* **116**, 6790 (2019).
- [43] H. Wang, A. Abhilash, C. S. Chen, R. G. Wells, and V. B. Shenoy, Long-range force transmission in fibrous matrices enabled by tension-driven alignment of fibers, *Biophys. J.* **107**, 2592 (2014).
- [44] A. J. Licup, S. Munster, A. Sharma, M. Sheinman, L. M. Jawerth, B. Fabry, D. A. Weitz, and F. C. MacKintosh, Stress controls the mechanics of collagen networks, *Proc. Natl. Acad. Sci. USA* **112**, 9573 (2015).
- [45] S. Münster, L. M. Jawerth, B. A. Leslie, J. I. Weitz, B. Fabry, and D. A. Weitz, Strain history dependence of the nonlinear stress response of fibrin and collagen networks, *Proc. Natl. Acad. Sci. USA* **110**, 12197 (2013).
- [46] O. V. Kim, R. I. Litvinov, J. W. Weisel, and M. S. Alber, Structural basis for the nonlinear mechanics of fibrin networks under compression, *Biomaterials* **35**, 6739 (2014).
- [47] M. Gardel, J. H. Shin, F. MacKintosh, L. Mahadevan, P. Matsudaira, and D. A. Weitz, Elastic behavior of cross-linked and bundled actin networks, *Science* **304**, 1301 (2004).
- [48] Y.-C. Lin, N. Y. Yao, C. P. Broedersz, H. Herrmann, F. C. MacKintosh, and D. A. Weitz, Origins of elasticity in intermediate filament networks, *Phys. Rev. Lett.* **104**, 058101 (2010).
- [49] I. K. Piechocka, R. G. Bacabac, M. Potters, F. C. MacKintosh, and G. H. Koenderink, Structural hierarchy governs fibrin gel mechanics, *Biophys. J.* **98**, 2281 (2010).

- [50] M. Jaspers, M. Dennison, M. F. Mabeoone, F. C. MacKintosh, A. E. Rowan, and P. H. Kouwer, Ultra-responsive soft matter from strain-stiffening hydrogels, *Nat. Commun.* **5**, 5808 (2014).
- [51] E. Conti and F. C. MacKintosh, Cross-linked networks of stiff filaments exhibit negative normal stress, *Phys. Rev. Lett.* **102**, 088102 (2009).
- [52] B. Burkel and J. Notbohm, Mechanical response of collagen networks to nonuniform microscale loads, *Soft Matter* **13**, 5749 (2017).
- [53] M. Wyart, H. Liang, A. Kabla, and L. Mahadevan, Elasticity of floppy and stiff random networks, *Phys. Rev. Lett.* **101**, 215501 (2008).
- [54] A. Sharma, A. J. Licup, K. A. Jansen, R. Rens, M. Sheinman, G. H. Koenderink, and F. C. Mackintosh, Strain-controlled criticality governs the nonlinear mechanics of fibre networks, *Nat. Phys.* **12**, 584 (2016).
- [55] C. P. Broedersz, M. Sheinman, and F. C. MacKintosh, Filament-length-controlled elasticity in 3D fiber networks, *Phys. Rev. Lett.* **108**, 078102 (2012).
- [56] D. A. Head, A. J. Levine, and F. C. MacKintosh, Mechanical response of semiflexible networks to localized perturbations, *Phys. Rev. E* **72**, 061914 (2005).
- [57] L. Liang, C. Jones, S. Chen, B. Sun, and Y. Jiao, Heterogeneous force network in 3D cellularized collagen networks, *Phys. Biol.* **13**, 066001 (2016).
- [58] A. Abhilash, B. M. Baker, B. Trappmann, C. S. Chen, and V. B. Shenoy, Remodeling of fibrous extracellular matrices by contractile cells: predictions from discrete fiber network simulations, *Biophys. J.* **107**, 1829 (2014).
- [59] H. Kang, Q. Wen, P. A. Janmey, J. X. Tang, E. Conti, and F. C. MacKintosh, Nonlinear elasticity of stiff filament networks: Strain stiffening, negative normal stress, and filament alignment in fibrin gels, *J. Phys. Chem. B* **113**, 3799 (2009).
- [60] P. Rosakis, J. Notbohm, and G. Ravichandran, A model for compression-weakening materials and the elastic fields due to contractile cells, *J. Mech. Phys. Solids* **85**, 16 (2015).
- [61] J. Notbohm, A. Lesman, P. Rosakis, D. A. Tirrell, and G. Ravichandran, Microbuckling of fibrin provides a mechanism for cell mechanosensing, *J. R. Soc. Interface* **12**, 20150320 (2015).
- [62] P. Ronceray, C. P. Broedersz, and M. Lenz, Fiber networks amplify active stress, *Proc. Natl. Acad. Sci. USA* **113**, 2827 (2016).
- [63] X. Xu and S. A. Safran, Nonlinearities of biopolymer gels increase the range of force transmission, *Phys. Rev. E* **92**, 032728 (2015).
- [64] L. M. Sander, Alignment localization in nonlinear biological media, *J. Biomech. Eng.* **135**, 071006 (2013).
- [65] P. Ronceray, C. P. Broedersz, and M. Lenz, Stress-dependent amplification of active forces in nonlinear elastic media, *Soft Matter* **15**, 331 (2019).
- [66] C. P. Broedersz, X. Mao, T. C. Lubensky, and F. C. MacKintosh, Criticality and isostaticity in fibre networks, *Nat. Phys.* **7**, 983 (2011).
- [67] Y. Fung, Elasticity of soft tissues in simple elongation, *Am. J. Physiol.* **213**, 1532 (1967).
- [68] T. Gutsmann, G. E. Fantner, J. H. Kindt, M. Venturoni, S. Danielsen, and P. K. Hansma, Force spectroscopy of collagen fibers to investigate their mechanical properties and structural organization, *Biophys. J.* **86**, 3186 (2004).
- [69] M. Das, D. Quint, and J. Schwarz, Redundancy and cooperativity in the mechanics of compositely crosslinked filamentous networks, *PLoS ONE* **7**, e35939 (2012).
- [70] M. Sheinman, C. P. Broedersz, and F. C. MacKintosh, Non-linear effective-medium theory of disordered spring networks, *Phys. Rev. E* **85**, 021801 (2012).
- [71] J. Xia, L.-H. Cai, H. Wu, F. C. MacKintosh, and D. A. Weitz, Anomalous mechanics of Zn<sup>2+</sup>-modified fibrin networks, *Proc. Natl. Acad. Sci. USA* **118**, e2020541118 (2021).
- [72] V. Panzetta, S. Fusco, and P. A. Netti, Cell mechanosensing is regulated by substrate strain energy rather than stiffness, *Proc. Natl. Acad. Sci. USA* **116**, 22004 (2019).
- [73] O. Chaudhuri, L. Gu, D. Klumpers, M. Darnell, S. A. Bencherif, J. C. Weaver, N. Huebsch, H.-p. Lee, E. Lippens, G. N. Duda *et al.*, Hydrogels with tunable stress relaxation regulate stem cell fate and activity, *Nat. Mater.* **15**, 326 (2016).
- [74] F. Guilak, D. M. Cohen, B. T. Estes, J. M. Gimble, W. Liedtke, and C. S. Chen, Control of stem cell fate by physical interactions with the extracellular matrix, *Cell Stem Cell* **5**, 17 (2009).
- [75] B. C. Isenberg, P. A. DiMilla, M. Walker, S. Kim, and J. Y. Wong, Vascular smooth muscle cell durotaxis depends on substrate stiffness gradient strength, *Biophys. J.* **97**, 1313 (2009).
- [76] See Supplemental Material at <http://link.aps.org/supplemental/10.1103/PhysRevResearch.6.013327> for additional robustness, finite size effects and buckling zone characterization, as well as details on experimental measurements.
- [77] K. A. Jansen, R. G. Bacabac, I. K. Piechocka, and G. H. Koenderink, Cells actively stiffen fibrin networks by generating contractile stress, *Biophys. J.* **105**, 2240 (2013).
- [78] H. Yang, E. Berthier, C. Li, P. Ronceray, Y. L. Han, C. P. Broedersz, S. Cai, and M. Guo, Local response and emerging nonlinear elastic length scale in biopolymer matrices, *Proc. Natl. Acad. Sci. USA* **120**, e2304666120 (2023).
- [79] L. D. Landau, E. M. Lifšic, E. M. Lifshitz, A. M. Kosevich, and L. P. Pitaevskii, *Theory of Elasticity* (Elsevier, Amsterdam, 1986), Vol. 7.
- [80] N. Q. Balaban, U. S. Schwarz, D. Riveline, P. Goichberg, G. Tzur, I. Sabanay, D. Mahalu, S. Safran, A. Bershadsky, L. Addadi *et al.*, Force and focal adhesion assembly: A close relationship studied using elastic micropatterned substrates, *Nat. Cell Biol.* **3**, 466 (2001).
- [81] J. P. Winer, S. Oake, and P. A. Janmey, Non-linear elasticity of extracellular matrices enables contractile cells to communicate local position and orientation, *PLoS ONE* **4**, e6382 (2009).
- [82] A. I. Athamneh and D. M. Suter, Quantifying mechanical force in axonal growth and guidance, *Front. Cell. Neurosci.* **9**, 359 (2015).
- [83] U. S. Schwarz and S. A. Safran, Physics of adherent cells, *Rev. Mod. Phys.* **85**, 1327 (2013).
- [84] A. Saez, A. Buguin, P. Silberzan, and B. Ladoux, Is the mechanical activity of epithelial cells controlled by deformations or forces? *Biophys. J.* **89**, L52 (2005).
- [85] A. K. Yip, K. Iwasaki, C. Ursekar, H. Machiyama, M. Saxena, H. Chen, I. Harada, K.-H. Chiam, and Y. Sawada, Cellular response to substrate rigidity is governed by either stress or strain, *Biophys. J.* **104**, 19 (2013).
- [86] <https://zenodo.org/records/10567423>